

THE ROYAL INSTITUTION OF NAVAL ARCHITECTS

OFF-WIND SAIL PERFORMANCE PREDICTION AND OPTIMISATION

A M Wright and A R Cloughton, Wolfson Unit MTIA, University of Southampton, UK
J Paton and R Lewis, TotalSim, UK

SUMMARY

The paper describes the current state of art for obtaining force coefficients for VPP calculations and surface pressure distributions for aero-elastic design. The methods appraised are parametric VPP force models, physical model testing in wind tunnel facilities, and the use of CFD from simple panel codes to RANS and DES simulations. The relative merits of the various options available to yacht, mast and sail designers are discussed in terms of complexity, cost and time-scale. The objective of this paper is to guide sail and yacht designers through the techniques available for the analysis and optimisation of off-wind sail plans and the rationale of the different approaches.

NOMENCLATURE

ν	Kinematic viscosity (N s m^{-2})
ρ	Density of water (kg m^{-3})
v	velocity (m s^{-1})
β / AWA	Apparent wind angle
L	Representative length of object(m)
P	Pressure (N m^{-2})
Rn	Reynolds Number (vL/ν)
q	dynamic pressure head (N m^{-2})
REEF	Sail area reduction factor
FLAT	Sail Lift reduction Factor
TWA	True Wind Angle
TWS	True Wind Speed
VPP	Velocity Prediction Program

1. INTRODUCTION

The efficient optimisation of a yacht and its sail wardrobe in a competitive environment requires the use of a wide range of tools and techniques. In addition to yacht and sail designers, the designers of the rig and rigging desire greater information as to the requirements, loads and performance of the sails. Off-wind sails are no longer purely drag devices and the detailed knowledge of separation zones and pressure distributions are essential.

Traditionally sail makers and designers delivering new sails have the following priorities, in descending order of importance

- The sail sets correctly
- The sail is strong enough
- The sail is fast

Generally the first issue is resolved as soon as the sail is sheeted on, while the second takes a few more hours. The concern of peak performance *may* be resolved before the sail is worn out.

Aspects of the problem that require consideration are different according to the apparent wind speed and angle range desired, as well as factors such as the size of the boat. A key consideration for all designs is to obtain an accurate flying shape. The ability to model and control different aspects of the wind (such as atmospheric

boundary layer, twist, unsteady velocity) all depend on the sail design requirements. For example, the influence of the atmospheric boundary layer upon a 12m LOA yacht travelling upwind is negligible compared to that upon a 35m LOA yacht reaching.

Another key driver for the selection of the most appropriate modelling method is the required data. A sail maker requires a pressure distribution map across the sail surface, whereas the yacht designer essentially requires driving force, heeling force and heeling moment for performance prediction.

There are a range of techniques that can be used to predict off wind sail performance, including theoretical, experimental and computational. Theoretical methods include the use of existing data and simplified formulae. Experimental testing usually implies wind tunnel testing of a scale model, measuring drive and heel forces, while there is a range of computational techniques allowing a balance of accuracy against computational cost. The computational codes in use for design purposes currently range widely between vortex lattice codes up to Detached Eddy Simulation (DES). Figure 1 presents typical computational effort requirements for a potential flow vortex lattice code, a Reynolds Averaged Navier-Stokes simulation (RANS) simulation and a DES simulation. This equates to a typical RANS turnaround

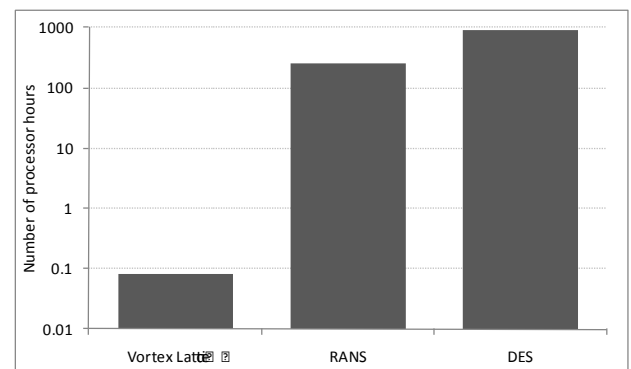


Figure 1 Computational effort required to obtain a solution

times of 5 hours for a 30 million cell model to automatically mesh and solve on 48 processors. DES time are approximately 3 to 4 times the RANS duration.

The use of a vortex lattice code is perfectly adequate for upwind design calculations but for close reaching and off-wind sails, the following points complicate the problem –

- The large separated wake
- The sail luff can be collapsed
- The Aero-elastic effects have strong interaction in terms of material deformation and unsteady behaviour
- The de-powering range of the sail to maintain a constant heel angle is greatly reduced

RANS solutions allow for viscous effects and separated flow via the use of turbulence models, but due to the nature of the mathematical formulation, any unsteady behaviour is not correctly modelled. More detailed simulations techniques, such as DES have been used to provide more accurate results for marine and other flows with significant zones of separated flow [1] [2].

2. WIND TUNNEL TESTING

2.1 FORCE MEASUREMENT

The most common approach to the set up of a sail testing dynamometer is described by Campbell [3]. The fundamental features of the force dynamometer are:

- the measured forces are those applied only to the mast, sails and hull of the model, hence the simple water seal arrangement,
- the dynamometer arrangement is configured to avoid significant interactions between the large heeling force and roll moment and the small driving force.

Typically forces are measured on the body axes of the hull, and transformed to the more tractable lift and drag forces in the apparent wind frame of reference. This requires high accuracy in model alignment and angle measurement.

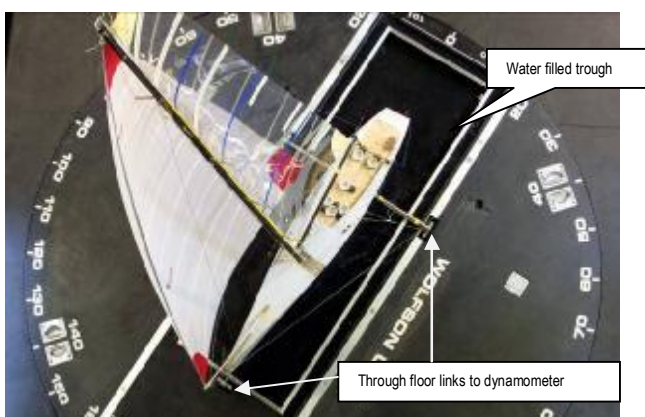


Figure 2 Typical wind tunnel set up

2.2 TESTING FLOW REGIME

Open jet wind tunnels, such as the University of Auckland TFWT as described by Le Pelley et al [4], can

use guide vanes to produce a “twisted” flow over the sails that mimics a twist profile i.e. a vertical variation of AWA with height. This feature is most useful when looking at reaching points of sailing (TWA 45-120 degrees). It is usual to set up a single “typical” twisted flow for the type of sails under investigation, and this allows the observed flying shapes to more closely represent those observed on the yacht. The flow is “twisted”, but not to match the exact profile for each combination of boat speed, wind speed and TWA.

Closed jet wind tunnels find it hard to introduce an onset flow over the model whose apparent wind angle varies with height. They do however allow force coefficients to be derived at an accurately determined q , in a consistent flow field.

The choice of facility probably depends on your geographical location and the type of work envisaged. Generally institutions are obliged to make a virtue out of necessity and play to the strengths of the facility they operate. The following section explores the techniques employed under the different test regimes.

2.3 WIND TUNNEL TEST METHODOLOGY

In the wind tunnel the model is set at a predetermined apparent wind angle, and during the tests there are usually two modes of sail trimming employed, “maximum power” and “de-powered”.

When “maximum power” testing the sail trimmer trims the sheets to achieve the maximum driving force and the resultant heeling moment is monitored. In VPP parlance this relates to REEF and FLAT being 1.00 [5]. Once the trimmer is happy that he has found a sail trim for maximum driving force the sheets can be eased, the traveller dropped to trim for the maximum available driving force at a range of steadily reducing heeling moment values.

Figure 3 shows typical data from individual test points from a wind tunnel test on different sail combinations over a range of apparent wind angles (25-80 degrees). The figure demonstrates several key features of data from tests on reaching sails.

- The available driving force increases with increasing apparent wind angle.
- At the smaller apparent wind angles the maximum driving force is approached asymptotically.
- De-powering, i.e. reducing heeling moment, can be achieved over a wider range when sailing close to the wind.
- At 50 degrees AWA, larger, more deeply cambered sails can be set, which increase both driving force and heeling moment.

At lower apparent wind angles the heeling moment can be reduced to approximately 50% of the maximum value by adjusting the main and fore-sail

sheets, without making substantial changes to mast tune and sail camber. The main deliverable from the tests at reduced heeling moment for upwind and close fetching points of sailing is the determination of the induced drag component. In this regime the drag varies with the square of the lift and an “effective rig height” can be derived.

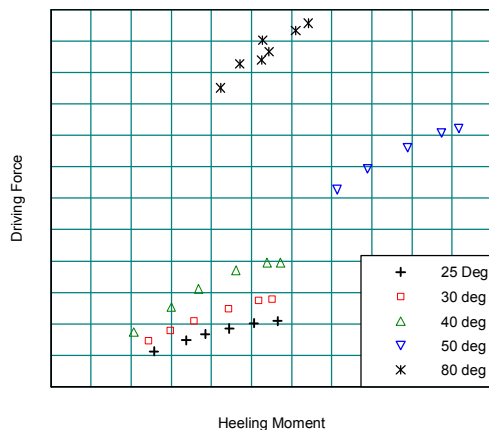


Figure 3 Typical Heeling Moment vs. Driving Force data from wind tunnel tests.

For reaching sails the techniques are similar, but once flying luff sails are under test the ability to de-power, i.e. reduce heeling moment, by easing the sheets is limited by the sail collapsing. For asymmetric spinnakers the moment reduction may be only 10-15% before the sail collapses, making it impossible to reliably determine an induced drag component. Teeters et al [6] present data on this type of testing to derive a more realistic force model for the IMS VPP.

2.4 TYPICAL RESULTS

Figure 4 shows typical heeling moment vs. driving force results for tests on a sloop at 40 degrees AWA. The data is for a range of headsails, from masthead Code zero (squares) to a Flying Jib (triangles) with full and reefed mainsail (green and cyan curves respectively). In order to determine which sails can be flown in what wind speed the heeling moment at a nominal maximum heel angle is calculated from the hull data. This line of maximum tolerable heeling moment (thick blue line) is plotted against true wind speed in knots (right hand axis)

For example, in 10 knots TWS the heeling moment limit is approximately 11 and only sail data points to the left of the vertical line at that Heeling moment can be used. If the true wind increases to 20 knots the vertical line shifts to around 3, and only reduced sail configurations can be contemplated.

The data also show where there is a wind speed gap in a particular wardrobe. On the plot the red crosses were never tested, they are an imaginary sail conceived to fill the dip between the code zero’s and the jibs. If the yacht characteristics change this type of plot can be used with

an alternative heeling moment limit line, and the new sail ranges determined.

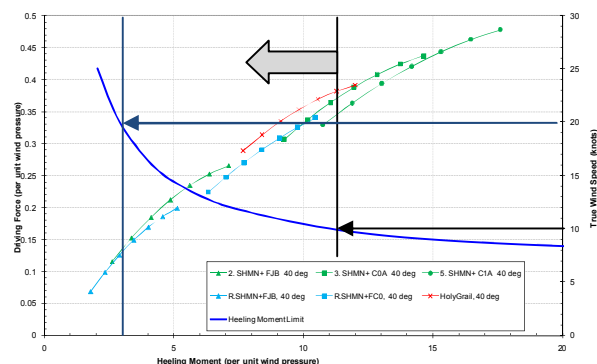


Figure 4 Typical wind tunnel results at 40 deg AWA

Where specific sail designs are tested it is common to use a “real time VPP” to trim the sails. The forces from the dynamometer are linked to a hydrodynamic force model for the hull, so sail choice and trimming strategies can be evaluated with reference to a real time prediction of boat speed and heel angle and rudder angle. This technique can also be extended to link the heel angle on the model to that predicted by the VPP, in this way as the sail sheet is pulled in the model heel angle will increase, in this way subtleties of the heel/driving force interaction are immediately apparent.

This gives the sail designer instant results on particular sail wardrobes, but the test results are inevitably boat design and stability specific. This is analogous to the situation in tank testing in the last century when the Wageningen tank adopted a procedure to test ballasted models towed from the top of a mast in the model to simulate real sailing conditions. The test results were specific to that boats stability curve and analysing the results to generate data that was useful in the general case becomes quite difficult.

2.5 DATA MAPPING FOR THE VPP

The data analysis required is related to the type of tests and the requirements of the end user.

For a sail designer looking at alternative sails for say a VO70 then he is often happy to leave a test session knowing only which design was fastest. On the other hand a researcher trying to codify offwind sail performance for general VPP use is faced with a more difficult task. The data must be corrected for blockage and analysed in such a way that it fits the aerodynamic force model paradigm. [6] [7]

Half way between these two extremes lies the development of sail wardrobes for say a multi-masted superyacht, such as that shown in Figure 5. Here a range of sail plans, including full hoist and reefed configurations are tested, each at a range of AWA, and looking for full power and reduced heeling moment data. These results are also affected by any sheeting

limitations imposed by the deck and stay topography. Indeed it is one of the most useful aspects of this testing to work out sail interaction effects and where rigging geometry might impair performance.



Figure 5 Typical multi-sail wind tunnel set up. (Courtesy Hoek Design).

2.5 (a) Experimental data fits.

To manage this type of data the Wolfson Unit developed a general format for an experimentally derived aerodynamic force model, (.AEX file). Because many of the sail trims tested in the wind tunnel are non optimum there is little point in having the VPP predict performance for these points. Similarly in some areas of the test matrix data may be sparse, and slavish point wise evaluation of the data would be unhelpful. Hence the AEX file was developed to capture the driving features of a sailplan for easy input to the VPP.

Figure 6 shows typical wind tunnel test data for two sail plans over a range of apparent wind angles. The data are plotted as driving force vs. heeling moment. The continuous blue and red “envelope curves” capture the maximum driving force points and the associated heeling moment. The few points outside the envelope are “over trimmed” points where driving force is actually falling with increasing heeling moment.

The faired lines through the points of reducing heeling moment at each apparent wind angle are derived from the values of effective rig height and vertical centre of effort position contained in the AEX file. Also mapped is the lowering of the centre of effort height as the sails are depowered. A similar “twist” factor is incorporated in the ORCi VPP. [8]

These values are obtained from an interactive analysis, fitting and faired tool developed to post process data from sail tests.

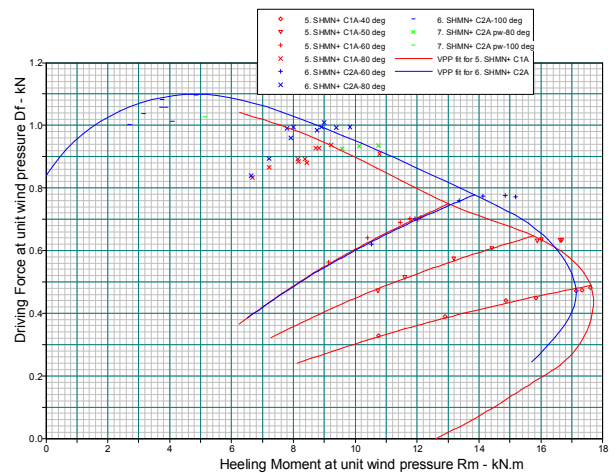


Figure 6 Driving force v. Heeling moment plot

The VPP can now use the AEX file data to determine an aerodynamic lift and drag force at any combination of AWA and AWS. Naturally it is as well to check the VPP is not using solutions that are too far away from the tested wind angles.

An AEX file is typically compiled from perhaps 100 test points for a baseline condition and 20-50 points for variations on a theme, but as previously stated you need to apply some manual filtering and expression to get a good result. In addition, the data must be stripped of hull windage drag otherwise the flattening algorithm will be incorrect. The windage forces are re applied during the VPP solution.

2.5 (b) CFD data fits

This analysis of experimental data is somewhat at odds with the requirements for data derived from CFD. It is (currently) inconceivable that you would make 200+ CFD runs, of which 70% were non optimum. With CFD the aim is to capture “perfect” sail sets and have the VPP sail at these points.

This is easier said than done because it’s the boat that decides the apparent wind angle, speed and twist. The best way to initialise CFD runs is to run a parametric VPP to determine the map of boat speed, AWA and, most importantly, the rolling moment through the wind speed range. Given this map the sail designer can build a rig and sails and start to trim them in a panel code which is almost instantaneous to run, (e.g. North Sails “Flow” or Azure Project vortex lattice). The flying shape of the sails can be adjusted so that the heeling force produced by the sails matches the sailing point. If this process is repeated at a range of AWA’s and range of wind speeds, then the VPP will find sailing balance points that are close to the CFD “results points”. If they are not then the process must be repeated with the sail trim adjusted. For CFD data analysis the VPP fitting is not about condensing 200 points into a useable file, its about

predicting boat speed with the sails set as the computer saw them.

The user now has 10-12 data points and needs the VPP to solve as close as possible to these points. A new method has been developed to use this type of data in the VPP, using an AEK file, which again is a simple text file of the CFD predictions of sail force and moment.

Although 'A-sails' are developed with a true wind speed or apparent wind speed in mind, for use in the VPP the force and moments from CFD will be normalized by dynamic pressure q and a reference area. So in the VPP "pipeline" they will certainly end up as drag and lift coefficients for a given apparent wind angle AWA .

Thus for a CFD run i , the essential result is force and moment coefficients F_i^j ($j=1, 6$) about the principal boat axes for a reference apparent wind angle β_i . Ideally this run is associated with a set of parameters for the rig and sail settings. These parameters for a typical rig might be main camber and twist, jib camber, traveller and jib track position.

This provides an apparent wind angle and some normalised force and moment data. With a proscribed set of apparent wind speeds (AWS) - a list of nominally ten AWS's ranging from 2 to 29 knots- a series of "back-calculations" are completed in the VPP to arrive at solutions (TWA, TWS, boat speed, heel angle). This equilibrates at the apparent wind angle (from CFD solution), and our list of AWS's. Now we have a set of VPP solutions for this single CFD solution. However, the various solution TWS/TWA sets will not necessarily coincide with the standard matrix of true wind speeds and angles in the VPP.

If only a speed and heel angle are required, then one could perhaps fit a surface to the solution data and interpolate the data from the surface. However, there are over 100 variables of interest that are associated with a single VPP solution, related to hydrodynamics, aerodynamics and other solution data, which would be lost with this interpolation method.

With this new approach the back solutions for 20 CFD points with 10 AWS's provide 200 solution points which are spread through the range of standard TWS's and TWA's. Finally the standard (TWS, TWA) pairs that fit within this cloud of CFD solution points are found, and then "forward solutions" using the CFD data for the standard matrix are completed. This is easier if the CFD solutions have been run with AWA sweeps of three or more angles. If not, then it is possible to overlay the VPP's internal aerodynamic coefficients as calculated for this sail/sailset onto this single AWA solution from CFD.

Finally, the VPP will filter for the "best" runs, and we can see which sail trimming or sail design parameters associated with each CFD run are producing the best

speeds. Although there are a number of other details with respect to wind gradient and twist, the approach results in a useful and efficient VPP solution for user-defined sail shapes that can work with a limited number of CFD data points.

Generating CFD results that match as closely as possible the actual sailing conditions of the boat is a big challenge. The sail trimmer sitting in front of his design computer knows nothing about what forces he needs to generate until the hull hydrodynamics and righting moment are known and interpreted through a VPP

3. COMPUTATIONAL COMPARISON

While vortex lattice results provide answers quickly, they lack the ability to model separation zone and arbitrary vortex formations correctly. Figure 7 presents the pressure distribution over a code 0 sail (Boat Speed 9.8 knots, TWS 8 knots, TWA 90), as calculated by a vortex lattice code and using RANS. The RANS solution was relatively low resolution (4 million cells), and took one hour on 24 processors of the University of Southampton's Iridis 3 cluster. While the overall pressure distribution is similar, the presence of a vortex off the foot of the sail is not predicted by the vortex lattice code and the pressure peak near the luff of the sail does not have the same level of variation with height compared to the RANS solution.

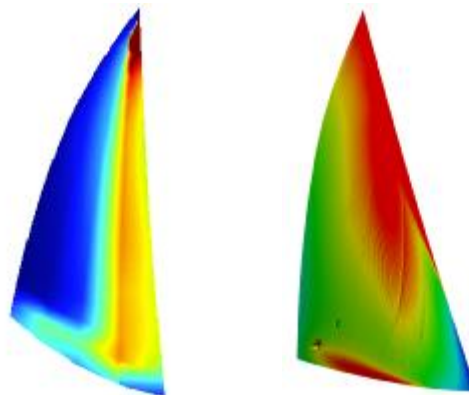


Figure 7 Comparison of pressure distribution from vortex lattice solution (left) with RANS solution

Even on this simple graphic it is clear that whilst the vortex lattice result is perfectly adequate for initial sail load calculations, it is not sufficient to derive real flying shapes and reliable driving force coefficients.

The following section compares two varying approaches to numerical modelling and CFD. The first will be that of steady-state RANS based modelling and the second being a transient DES approach. The results are compared and discussion is offered as to their ability to aid in the design cycle. As a test case a simplified hull, with mainsail and code zero sail have been modelled (note that this is a different test case to that modelled by

the vortex lattice code above). The parameters of the case study are listed in Table 1.

Boat Speed	11.8 knots
TWA	147 degrees
TWS	14 degrees
Heel	15 degrees
Zref	10m

Table 1 Off wind test case

3.1 RANS SIMULATION

RANS based approaches to aerodynamic problems are now common place in many sectors, including the automotive industry where their part in the design cycle is routine. The most common approach to RANS modelling is with the use of two equation models, including the $k - \epsilon$ and $k - \omega$ models which have become industry standards. By definition, two equation models include two extra transport equations to represent the turbulent properties of the flow.

One of the assumptions made in simplifying the full Navier-Stokes equations for this type of RANS approach is that of isotropic turbulence. This approximation can be valid in simplified applications, but becomes less valid for real world engineering applications with swirling flows.

3.1 (a) Model set up

The RANS model created for this example was meshed and solved within OpenFOAM [9] developed and maintained by OpenCFD Ltd.

The mesh used for the simulations, was created using snappyHexMesh within OpenFOAM. This is an automated fully hexahedral mesher. The geometry was placed in a domain 360m in length, 160m wide and 120m high. Approximately 30 million cells were used within this study. Surface refinement, proximity refinement and 'wake blocks' were used to control volume and surface mesh sizes. Surface layers were used to control cells within the boundary layer. Due to the nature of the meshing algorithm, snappyHexMesh is able to deal with complex geometries and scanned surfaces quickly and easily. Figure 8 show this ability to *automatically* mesh complex 'real world' geometries.

To model the wind twist for off-wind and downwind sails a twisted wind model was developed. This was then applied to 3 surfaces to create an inlet/outlet surface depending on whether the flow is entering or leaving the domain. One of the domain walls was set as an outlet. The domain bottom/sea was set as a wall with velocity equal to that of the boat speed. The top surface was set as a symmetry plane.

One of the advantages of a fully hexahedral mesh is the removal of mesh diffusion. The hexahedral mesh structure helps maintain the boundary layer profile.



Figure 8 Example surface mesh showing the level of automated detail refinement possible

Figures 9 and 10 help demonstrate the ability of OpenFOAM to maintain the boundary layer applied at the inlets. Figure 9 shows visually the boundary layer across the domain. Within this example the flow is travelling through the domain from left to right. The left surfaces are inlets whilst the right surfaces are outlets, with near identical boundary layer profiles. Figure 10 is an extract from the boundary layer profile on the far side of the domain/outlet, comparing the actual velocity profile to that of the analytical numbers applied to the inlet. The differences in profile occurring mainly due to the steps in mesh size, where the velocity gradients are highest near the surface.

The model was solved within OpenFOAM using a TotalSim modified version of the solver. The SST (shear stress transport) turbulence model was used with lookup wall functions to model the near wall flow. A steady state simulation was created with averaging of coefficients and forces over time to monitor convergence and for comparison to the DES results.

The simulation took approximately 5 hours to mesh and solve on 48 i7 2.66 GHz processors with 288 GB of RAM. The solve time in isolation was approximately 4 hours.

3.1 (b) Modelling Issues

One of the complex features for the numerical set up is the ability to accurately model the wind twist. For cases with significant amounts of wind twist (>90 degrees), difficulties in setting inlet/outlet boundary conditions can occur. For example, a case with a large amount of twist may result in a wall acting as an inlet or outlet at different heights through the domain. The ability of OpenFOAM to set these complex boundary conditions without having to change meshing recipes, for varying twist, simplifies this process.

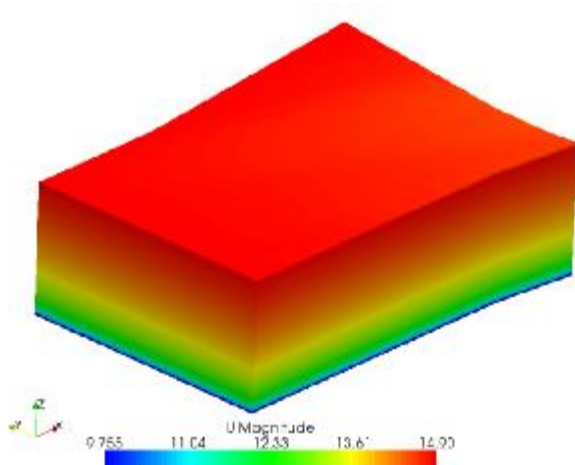


Figure 9 Example boundary layer profile throughout the domain

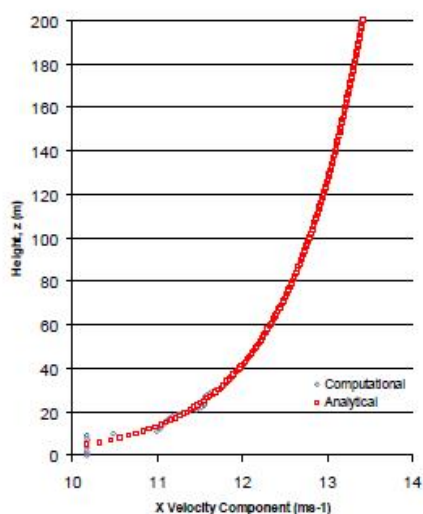


Figure 10 Example boundary layer profile

The main issue surrounding the use of many RANS models including the SST turbulence model, is their dependency upon the Boussinesq assumption. This assumption states that Reynolds stress tensor is proportional to the mean strain rate tensor, by introducing a new term eddy viscosity. The most common RANS models are two equation models which fail to account for turbulence anisotropy. This assumption is a large simplification which helps reduce run and turn around times but its accuracy in real world complex flows is limited. Without doubt the modelling of offwind sails using steady state RANS models has its limitations. Its place within the design cycle is discussed later.

3.1 (c) Results for RANS test case

Shown in Figure 11 is the force convergence plot for the RANS simulation, showing drag and side forces vs iteration. Here it can be seen that by 3000 iterations the forces have stabilised.

Table 2 shows the breakdown of forces from the RANS approach, averaged over final 500 iterations. Here it can be seen that the ~1000N of total driving force is created with ~200N from the mainsail and ~870N from the foresail whilst the hull created the remainder of the drag. The total side force of ~1300N is created from a ~300N contribution from the mainsail and ~1000N contribution from the foresail. Further discussion of the forces and post processing images are given later with comparison to the DES results.

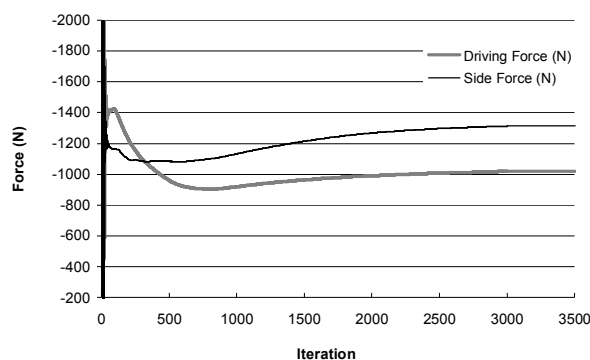


Figure 11 RANS force convergence

3.2 DES SIMULATION

Detached eddy simulation (DES) is a method that combines Large Eddy Simulation (LES) and RANS solvers. Regions near solid boundaries and where the turbulent length scale is less than the maximum grid dimension are assigned the RANS mode of solution. As the turbulent length scale exceeds the grid dimension, the regions are solved using the LES mode. Therefore the grid resolution is not as demanding as pure LES, thereby considerably cutting down the cost of the computation. Therefore DES is potentially more accurate but at an added computational costs.

3.2 (a) Set up

The DES model was 'run-on' from the converged RANS model to help reduce run times and increase stability. The DES model used was the SpalartAlmarasDDES model within OpenFOAM.

An adjustable time step was used based upon a maximum Courant number, set to 3, which equated to a physical time step of approximately 0.001s. Ten seconds of simulation took approximately 10 hours on 48 i7 2.66 GHz processors. The model was solved using an inhouse evolution of the OpenFOAM solver pimpleFoam. For comparison to the RANS model and to monitor convergence, time averaging of the forces was conducted.

3.2 (b) DES modelling issues

The use of the DES model has certain advantages and disadvantages over the RANS based model. Many of the issues surrounding the RANS based model demonstrated earlier, including the unsteady and isotropic turbulence constraints have now been removed or relaxed. This has

the advantage of potentially more accurate simulations capable of more realistic transient analysis and capture of the larger eddies. This comes at the expense of CPU hours as shown in Figure 1.

3.2 (c) Results for the DES test case

Figure 12 presents the force convergence plot, showing drag and side forces vs iteration, over 15 seconds of simulation time. In contrast to the RANS solution there is an increase in the noise due the highly transient nature of the simulation. It is therefore essential that for accurate comparison time averaging of forces and pressures be carried out. In this example the forces were averaged over the final 5 seconds of the simulation.

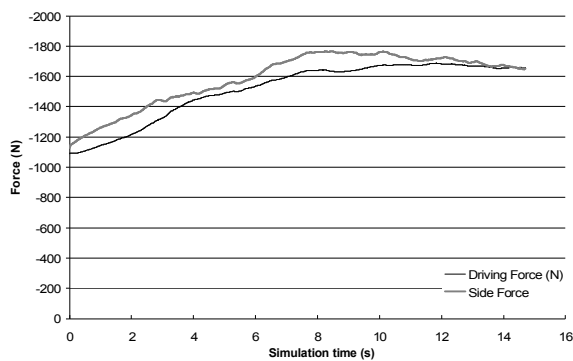


Figure 12 RANS force convergence

The increase in forces through the early stages of the DES simulation is evident. Further discussion and comparison between the forces and results will be given in the following section.

Table 2 shows the breakdown of forces from the DES approach, averaged over the final 5 seconds of simulation. Here it can be seen that the ~1670N of total driving force is created by ~250N from the mainsail and ~1430N from the foresail whilst the hull was creating a small amount of drag. The total side force of ~1700N is created from a ~430N contribution from the mainsail and ~1210N contribution from the fore-sail (Kite).

4. RANS vs DES Discussion

Two computational methods have been investigated in the previous sections, utilising RANS and DES approaches. Shown in Table 2 is a comparison of the forces between the two with absolute and percentage deltas. It is clear from this analysis that the difference between the two approaches is significant with differences in driving forces of 65% and 35% difference in side force. There is also a notable change in the drive to heel force ratio, from 0.78 to 0.98.

The main contributions to the increase in driving force come from increased foresail forces. The images in Figure 13 and 14 show surface contours of pressure coefficient and near wall velocity. On the left side of these Figures are the RANS results and the right side are the DES. To highlight the differences, instantaneous DES variables are shown rather than time averaged. The

reduction in leeward surface pressure is clear to see in addition to changes in near wall velocities. It can be seen in these images that the upper parts of the code zero are separated, shown by the low near wall velocity. It is worth noting again that the geometries shown here have in no way been optimised, but rather have been chosen to demonstrate the differences and capabilities between different methods.

	Total			main		
	Drag	Side Force	Vertical	Drag	Side Force	Vertical
RANS	-1013.5	-1304.6	154.2	-197.8	-298.4	-73.7
DES	-1669.1	-1702.6	163.9	-252.2	-428.2	-117.7
Delta	-655.6	-398.0	9.7	-54.4	-129.9	-44.0
Delta %	64.7%	30.5%	6.3%	27.5%	43.5%	59.8%
	kite			hull		
	Drag	Side Force	Vertical	Drag	Side Force	Vertical
RANS	-873.6	-991.6	181.2	57.9	-14.7	46.6
DES	-1433.6	-1208.8	242.5	16.6	-65.6	39.0
Delta	-560.0	-217.3	61.3	-41.2	-50.9	-7.6
Delta %	64.1%	21.9%	33.8%	-71.2%	346.4%	-16.4%

Table 2 Comparison of RANS and DES results

Figures 15 and 16 show isocontours of total pressure, which is the sum of the static and dynamic pressures. Total pressure contours can be used to show turbulent structures within the flow. The initial obvious difference is the unsteady nature of the DES contours in comparison to the RANS contours. This is due to many factors, including the transient nature of the simulation and the capture of the larger eddies. Another feature prominent in the isocontours of total pressure is the foot vortex shown in Figure 17. This is significantly more prominent at the foot of the foresail than it was with the RANS approach. It is possible that this large foot vortex is causing the significant reduction in pressure coefficient seen on the leeward side of the DES sail in Figure 13. The influence of this foot vortex can be seen in Figure 14 by the band of high velocity flow at the leech originated at the tack. However, it is difficult to say whether this vortex is a cause or effect and certainly needs further investigation. The question as to whether the foot vortex is causing the increase in low surface pressure on the leeward side or whether it is just the result of a larger pressure differential between the two sides of the sail is yet to be determined.

The differences in forces between RANS and DES is significant and needs to be further investigated. The potential for DES based modelling to replace RANS based models seems inevitable as computational resources increase. This will give the designer more accuracy, confidence and detail to better understand the flow around sails.

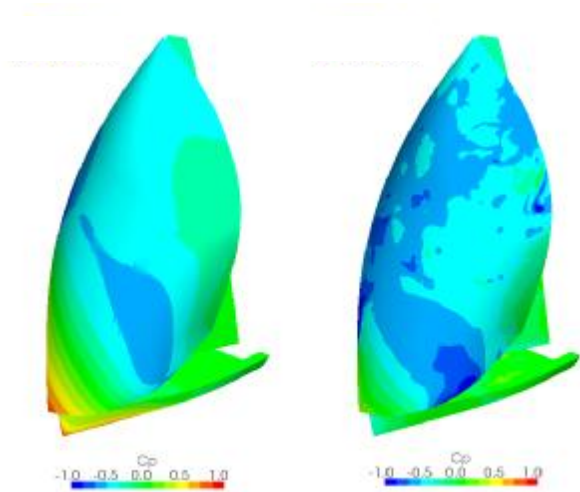


Figure 13 Surface pressure contours

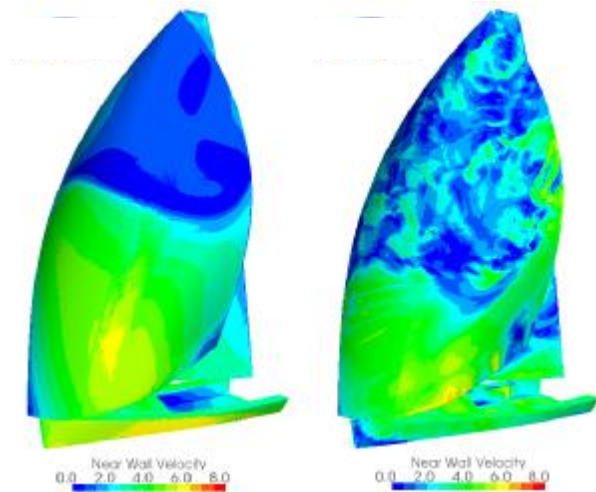


Figure 14 Surface near wall velocity contours

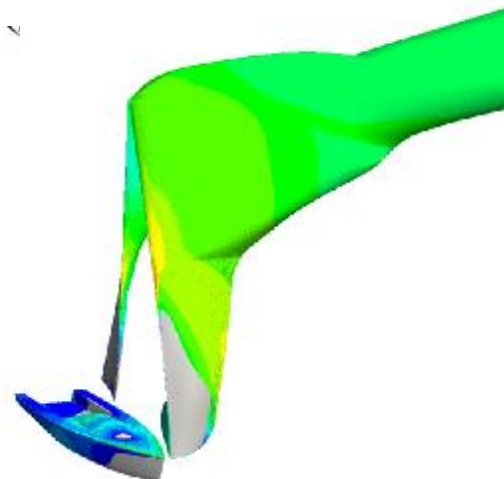


Figure 15 RANS total pressure contour coloured by velocity

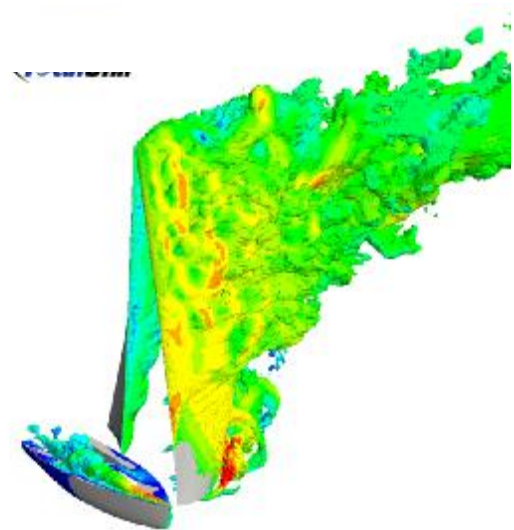


Figure 16 DES total pressure contour coloured by velocity

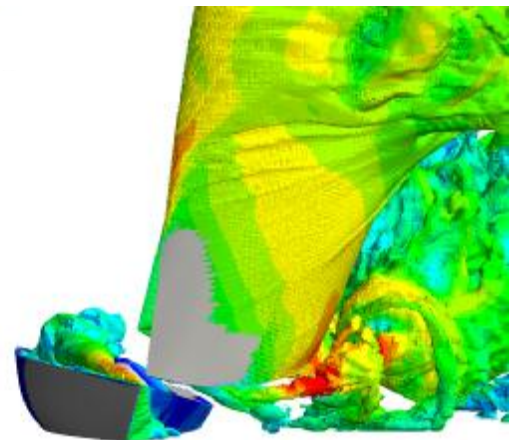


Figure 17 DES total pressure contour coloured by velocity showing foot vortex

5. CONCLUSIONS

Sail design and its integration into the related mast and hull design have developed significantly over the last two decades, mainly through the rapid cycle times of inviscid panel codes and structural analysis (e.g. Membrain or Relax). Issues of flying shape and structural integrity can now be reliably addressed at the design stage using inviscid codes. The techniques described in this paper have attempted to explore ways to predict optimum sail performance. Over time analytical techniques will gain more credence and wider use, particularly if the trend towards stringent sail limitations and restricted on the water testing windows as a cost control measure continues.

Whether inviscid codes will ever be removed completely from the design cycle is yet to be seen as their instantaneous turnaround times will continue to be key to the designer. The ability of DES to capture the transient and separated flows of off-wind sails could be paramount

in the accurate modelling and performance prediction of yachts for the future.

6. REFERENCES

1. Pattenden, R.J., Turnock, S.R. and Bressloff, N.W. (2004) "The use of detached eddy simulation in ship hydrodynamics. In, 25th Symposium on Naval Hydrodynamics, St. Johns, Canada, pp 1-19. August 2004
2. Pattenden, R.J., Bressloff, N.W., Turnock, S.R. and Zhang, X. "Unsteady simulations of the flow around a short surface-mounted cylinder". International Journal for Numerical Methods in Fluids, 53, (6), 895-914. 2007
3. Campbell I.M.C. "The performance of off-wind sails obtained from wind tunnel tests" R.I.N.A. International Conference on the Modern Yacht, March 1998
4. Le Pelley D, Ekblom P & Flay R. "Wind Tunnel Testing of Downwind Sails". The 1st International Conference on High Performance Yacht Design. December 2002 Auckland.
5. Ranzenbach R & Teeters J "Enhanced de-powering model for offwind sails". The 1st International Conference on High Performance Yacht Design. December 2002 Auckland.
- 6 Teeters, J., Ranzenbach, R. & Prince, M "Changes to sail aerodynamics in the IMS Rule" The 16th Chesapeake Sailing Yacht Symposium, March 2003
7. Ranzenbach, R. & Mairs C. "Experimental determination of sail performance and blockage corrections." The 13th Chesapeake Sailing Yacht Symposium, March 1997
8. Offshore Racing Congress International Technical Committee. "ORC VPP Documentation 2010"
<http://www.orc.org/>
9. OpenFOAM, www.openfoam.com, Accessed 25th May 2010.

7. AUTHORS BIOGRAPHY

Alexander Wright is currently a Senior Research Engineer at the Wolfson Unit. He gained a PhD in adaptive meshes for CFD, and has since worked in the fields of both experimental testing and computational modelling. He has contributed on projects including Volvo 70's, IMOCA 60's and the 2008 UK Olympic track cycling equipment development.

Andy Cloughton is a Principle Research Engineer at the Wolfson Unit and a member of the ORC International Technical Committee responsible for the VPP

calculations that support ORCi yacht race handicapping system. His previous experience includes the execution of model and full scale sailing trials and the development of sailing yacht performance prediction tools for the America's Cup, Volvo Ocean Race and IMOCA Open 60 yachts.

Jon Paton is a CFD engineer at TotalSim. He studied towards a PhD in modelling the Fluid Structure Interaction of yachts sails before joining TotalSim where he has working on a vast range of projects from Formula 1 and Le Mans racing car development to the modelling and optimisations of yachts and masts.

Rob Lewis is the managing director of TotalSim. Since completing his PhD at the University of Leeds he has worked on and led projects from all the major engineering disciplines.